Impact of real-time ionospheric determination on improving precise navigation with GALILEO and next-generation GPS

M.Hernández-Pajares, J.M.Juan, J.Sanz, *Research group of Astronomy and Geomatics, gAGE/UPC, Barcelona, Spain*
O.L.Colombo, *GEST/NASA GSFC Code 926, Greenbelt, Maryland, USA*

BIOGRAPHIES

Dr. Manuel Hernández-Pajares is associate professor of the Department of Applied Mathematics IV at the Technical University of Catalonia (UPC), from 1993. He started working on GPS in 1989, for cartographic and surveying applications. His focus has been in the area of GNSS atmospheric determination and precise radionavigation, since 1995.

Dr. J. Miguel Juan Zornoza is an associate professor of the Department of Applied Physics at the Technical University of Catalonia (UPC). His current research interest is in the area of GPS ionospheric tomography, GPS data processing algorithms, and radionavigation.

Dr. Jaume Sanz Subirana is an associate professor of the Department of Applied Mathematics IV at the Technical University of Catalonia (UPC). His current research interest is in the area of GPS ionospheric tomography, GPS data processing algorithms, and radionavigation.

Dr. Oscar L. Colombo works on applications of space geodesy, including gravity field mapping, spacecraft orbit determination, and precise positioning by space techniques, mostly for the Space Geodesy Branch (Code 926) of NASA Goddard Space Flight Center. In recent years, he has developed and tested techniques for very long baseline kinematic GPS, in collaboration with groups in Australia, Denmark, Holland, and the USA.

ABSTRACT

The ionospheric differential refraction, at distances of tens of kilometers or more, is one of the main problems affecting the capability of instantaneous carrier phase ambiguity resolution. And, as a consequence, the ionosphere affects the feasibility of centimeter-accuracy navigation with dual-frequency Global Navigation Satellite Systems such as present-day GPS, as well as future systems with three frequencies, like GALILEO and the Modernized GPS. We have shown in previous work that a real-time tomographic model of the ionosphere, computed from the GPS reference network data, is accurate enough to allow GPS real-time carrier phase ambiguity resolution for a rover at hundreds of kilometers from the nearest reference site. In this work, we study the extension of such techniques to the improvement of instantaneous three-carrier phase ambiguities resolution algorithms, such as TCAR, at medium and long distances (from tens to hundreds of kilometers), and with a minimum of geodetic computation. The data sets used have been generated with a modified GNSS satellite signal generator. In particular, improvements in the instantaneous ambiguity resolution success rate with three frequencies can be attained from about 60% of all attempts in previous work to about 100% with the proposed technique, at distances of about 60 km and with low ionospheric values, and to more than 90% at distances of more than 100 km under Solar Maximum conditions.

INTRODUCTION

Long-range, real-time, carrier-phase DGPS, with sub-decimeter precision and separations of up to several hundreds of kilometers between the rover and the nearest station, requires the estimation or resolution of the carrier-phase ambiguities and other unknowns to achieve high precision. Effects that tend to cancel out between receivers in short-baseline DGPS, remain quite significant in long-range DGPSs: Broadcast orbit errors, tropospheric refraction correction errors, and floated ionospheric-free combination (Lc) biases. These additional unknowns have to be estimated simultaneously with the position of the user's rover, in the navigation Kalman filter. This filter needs to receive and assimilate GPS data for a while, until it has enough to make precise estimates of all the unknowns. Until then, the position cannot reach the desired accuracy. This could take the better part of one hour, and is known as the convergence period of the filter. The main reason for this delay is the estimation of the floated Lc biases. If one could resolve the corresponding ambiguities and then use the result to eliminate the biases, the convergence period would be much shorter, and precise navigation could begin that much sooner (Colombo et al., 1999, 2000). This is the main reason for attempting to resolve ambiguities in long-range navigation.

The planned three-carrier satellite navigation systems offer the potential advantages of high success and integrity in instantaneous ambiguity resolution, with a minimum geodetic computation load. But it can be seriously affected by the ionospheric refraction, as is detailed below. Therefore, it makes sense to introduce an accurate modelling of the ionosphere in real time, as we have demonstrated in (Hernández-Pajares et al. 1999a, 2000 a, Colombo et al. 1999, 2000).

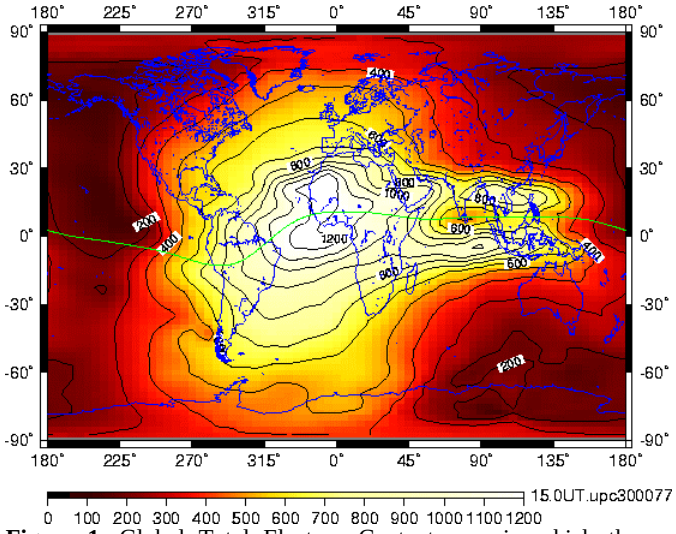

Figure 1: Global Total Electron Content map in which the vertical ionospheric delay, computed from actual GPS data, is represented for the target day of the experiment analyzed in this work, 17 March 2002 (units: 10^{-1} TECU = 1.6 cm in L1).

Several techniques have been proposed so far to improve the instantaneous positioning by using three-frequency systems, such as Three-Carrier Ambiguity Resolution, or TCAR, and Cascade Integer Resolution, or CIR (see for instance Vollath et al. 1998, Jung et al. 2000). They share a similar basic approach: the double differenced integer ambiguities are successively solved from the longest to the shortest beat-wavelength, including "extra-wide lane" and "wide lane" combinations of carrier phases (with wavelengths of 7.480m and 0.862m, respectively, in the datasets used in this work), and the first carrier L1 (with a wavelength of 0.190m).

But, in particular, TCAR performance is strongly affected by the ionospheric refraction decorrelation with distance. Indeed, as we will see, the ionosphere delay is a problem when its double differenced value is greater than 0.26 Total Electron Content Units (TECU)[1] (about 4 cm in L1). And typical values can exceed this threshold, as it is shown in the vertical ionospheric Total Electron Content (TEC) map computed from GPS data in figure 1. As a consecuence, an Integrated TCAR approach (ITCAR) has been developed by several authors (Vollath et al. 1998), including search algorithms and a navigation filter in which the ambiguities are part of the outputs and the ionospheric residual errors are coarsely estimated. But the ITCAR algorithm is still affected by the lack of knowledge of the double difference ionospheric refraction, limiting successful ambiguity resolution to cases where the separation between roving and fixed receivers is limited to a few tens of kilometers or more (Vollath et al. 2001).

In this paper, we extend our previous work on the application of real-time ionospheric corrections to ambiguity resolution. These corrections are generated in real time with a Kalman filter that assimilates dual-frequency carrier phase data from the network of reference stations. They are used to eliminate the effect of the ionosphere from the double-diferenced data, making it possible to resolve the ambiguities in real time, with dual-frequency systems such as GPS. One example is our Wide Area Real Time Kinematic (WARTK) method (Hernández-Pajares et al. 2000, 2001). These accurate ionospheric corrections can be broadcast to the users. In turn, these correct and then process their "ionosphere free" data to resolve their ambiguities with a simple algorithm such as TCAR . As we explain in this work, this approach (WARTK-3) produces a better performance at long distances from the nearest reference site than ITCAR, allowing the instantaneous resolution of more than 90% of ambiguities over baselines of more than 100 km. Moreover, WARTK-3 is a quite simple algorithm with a low computation load for the user, compared with ITCAR. Also WARTK-3 is simpler than the dual-frequency algorithm WARTK, that we shall explain briefly in the next section.

WARTK: PREVIOUS WORK WITH GPS

We have shown in previous work that a real-time tomographic model of the Ionosphere is accurate enough to solve On-The-Fly the GPS carrier phase ambiguities in a rover at hundreds of kilometers from the nearest reference site, using the corresponding reference network corrections (figure 2), generated with a combined ionospheric and geodetic filter (see Hernández-Pajares et al. 2000, 2001 for details). We have tried this form of ambiguity resolution for precise navigation, with sub-decimeter precision, and for making instantaneous atmospheric water-vapour determinations for meteorological applications, within wide-area networks with stations hundreds of kilometers apart. This approach fills the gap in the typical accuracy versus baseline length plot (see figure 3), between the Local Area DGPS (or GBAS) systems, with centimeter accuracy, but limited to distances below 20 km, and the new Global DGPS systems with sub-meter accuracy over thousands of kilometers (Bar-Sever et al., 2001).

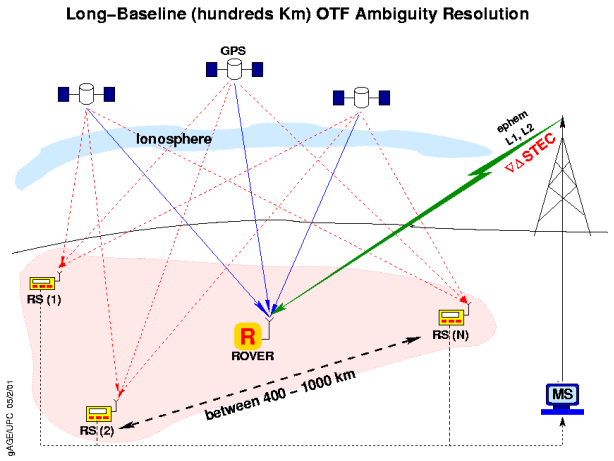

Figure 2: The Wide Area Differential GPS (WARTK) corrections, in particular the ionospheric ones, should be broadcast to the users.

[1] 1 TECU = 10^{16} electrons/m^2 ≈ 16.23 cm in L1

WARTK has been tested in different scenarios: under hard ionospheric conditions typical of Solar Maximum, during Ionospheric Storms, and in the presence of Travelling Ionospheric Disturbances ,TID's (Hernández-Pajares et al., 2001b). On the other hand, in the case of distances between stations of more than several hundred kilometers, strong electron content gradients can limit the performance of the technique. For this reason, an extension of the algorithm has been developed recently to include the case of reference stations separated thousands of kilometers (Hernández-Pajares et al. 2002).

ORIGINAL TCAR ALGORITHM FOR 3 FREQUENCY SYSTEMS

The planned three-frequency systems should offer more simultaneous observations, improving the chances of instantaneous (single epoch) ambiguity resolution, compared with the present dual-frequency GPS system. How this may work can be understood by studying one of the first algorithms proposed for 3 frequency navigation systems, the Three Carrier Ambiguity Resolution, or TCAR (Harris 1997). It consists of three basic steps:

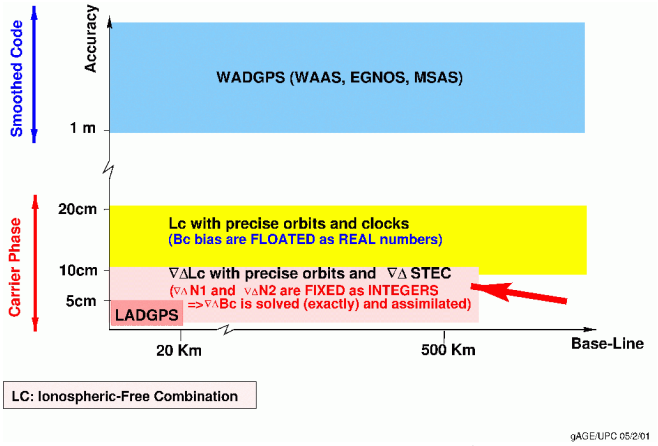

Figure 3: Accuracy versus baseline length (from the nearest reference site) plot for different GPS differential systems. The WARTK approach fills a gap, with subdecimeter errors at hundreds of kilometers baselines.

Step 1. Solve the extra-wide lane ambiguity (with a wavelength of ~7.45 meters in our dataset) by adding a pseudo-range combination. Although in some cases the pseudo-range multipath can diminish the chances for succes, this error is typically small compared with the long wavelength of the extra-wide lane, and can not present much of a problem.

The first step of the TCAR approach (see for example Vollath et al. 1998) is to estimate the double differenced (between pairs of receivers and satellites) ambiguities $\nabla\Delta N_{ew}$ of the double differenced extra-wide lane carrier phases $\nabla\Delta L_{ew}$, using a combination of pseudo-ranges (or codes) P_{ew} that share the same value and sign of ionospheric delay as the wide lanes. . This is possible due to the very long wavelength of the extra-wide lane combination, such the 7.45m in the case of the datasets generated for this study (Laboratory exp. 2000, and AGGA validation reports, 2000).

The corresponding equations are:

$$L_{ew} = \lambda_{ew}(\phi_3 - \phi_1) = \frac{f_3 L_3 - f_1 L_1}{f_3 - f_1} =$$

$$= \rho^* + \lambda_{ew} b_{ew} + \alpha_{ew} I + m_{ew} + \varepsilon_{ew} + \ldots \quad (1)$$

$$P_{ew} = \frac{f_3 P_3 + f_1 P_1}{f_3 + f_1} = \rho^* + \alpha_{ew} I + M_{ew} + \mathrm{E}_{ew} + \ldots \quad (2)$$

L_X being the carrier phase observation (in length units) of frequency f_X and wavelenght λ_X (see table 1 below), and P_X the corresponding pseudorange observation. The multipath and observation errors for carrier phases and pseudoranges are indicated by m_X, M_X and ε_X, E_X respectively (see maximum values of multipath and typical measurement errors in table 1). The indifferenced carrier phase ambiguity $\lambda_X b_X$, that contains instrumental delays and, after double-differencing, becomes an integer multiplier value of the wavelength, $\lambda_X \nabla\Delta N_X$. The ionospheric delay $\alpha_X I$ is multiple of the Slant Total Electron Content (STEC) I, the integrated free electron density along the ray that is usually measured in TECU units. The term ρ^* represents the terms that do not depend on the frequency (range, clock errors, tropospheric refraction, etc.).

	X=1	X=2	X=3	X=ew	X=w
f_X	1575.42	1227.6	1615.5	40.08	347.82
λ_X	0.1903	0.2442	0.1856	7.4799	0.8619
ε_X	≈0.002	≈0.002	≈0.002	≈0.1	≈0.01
E_X	≈1	≈1	≈1	≈1	≈1
m_X	<<0.05 (< 0.01)	<<0.06 (<0.01)	<<0.05 (<0.01)	<<2 (<0.5)	<<0.2 (<0.05)
M_X	<<450 (<10)	<<450 (<10)	<<450 (<10)	<<450 (<10)	<<450 (<10)
α_X	-0.1623	-0.2673	-0.1543	0.2083	0.2031

Table 1: The main numbers listed for the different kind of observations considered in this work, associated with the L1, L2, L3, and the extra-wide lane and wide lane carrier phases (Lew and Lw): Frequency (f_X, in MHz), wavelength (λ_X, in meters), Phase Measurement Error (ε_X, in meters), Code Measurement Error (E_X, in meters), Maximum and typical Phase Multipath (m_X, in meters) , Maximum and typical Code Multipath (M_X, in meters), and Ionospheric coefficient (α_X, in meters/TECU).

From the last equation, in which additional minor terms such as the carrier-phase wind-up are not explicitly written, it is possible to estimate the double-differenced extra-wide lane ambiguity $\nabla\Delta\hat{N}_{ew}$ in one epoch, substracting the corresponding code:

$$\nabla\Delta\hat{N}_{ew} = \frac{1}{\lambda_{ew}}\nabla\Delta\left(L_{ew} - P_{ew}\right) = \nabla\Delta N_{ew} - \\ -\frac{1}{\lambda_{ew}}\left(\nabla\Delta M_{ew} + \nabla\Delta \mathrm{E}_{ew}\right) + \ldots \quad (3)$$

In absence of severe multipath affecting the receivers (less than few meters), the error term of such estimation, taking also into acount the measurement error, is less than 0.5 cycles (about 3.5 meters), allowing the ambiguity to be fixed to the right integer value instantaneously.

Step 2. The wide lane combination ambiguity (equation 4) is estimated from the unambiguous extra-wide lane carrier phase obtained in step 1. The difference between them consists mostly of the wide lane ambiguity, and the differential ionospheric refraction (about 0.06 cycles/TECU with our work frequencies). The non-dispersive terms cancel out (equation 5). The main problems here are the measurement error and multipath in the carrier phase signals. Although typical values of differential ionospheric refraction at mid-latitudes and baselines below 100 km are just few TECU, the use of an ionospheric correction can significantly increase the success percentage at longer distances, and in more difficult ionospheric scenarios.

Once the first long-wavelength ambiguities $\nabla\Delta N_{ew}$ are solved by using the corresponding pseudoranges, a second 'mid-wavelength' ambiguity such as the wide lane combination,

$$L_w = \lambda_w(\phi_1 - \phi_2) = \frac{f_1 L_1 - f_2 L_2}{f_1 - f_2} = \\ = \rho^* + \lambda_w b_w + \alpha_w I + m_w + \varepsilon_w + \ldots \quad (4)$$

can be estimated from $\nabla\Delta N_{ew}$ and from the corresponding difference of carrier phases (see corresponding constant values in table 1):

$$\nabla\Delta\hat{N} = \frac{1}{\lambda_w}\nabla\Delta(L_w - L_{ew} + \lambda_{ew}N_{ew}) = \nabla\Delta N_w + \\ -\frac{1}{\lambda_w}\nabla\Delta(\varepsilon_{ew} + m_{ew} - m_w) + \frac{1}{\lambda_w}(\alpha_w - \alpha_{ew})\nabla\Delta I \quad (5)$$

In the presence of moderate multipath, the corresponding error term of the last expression that also includes the observational error is usually lower than 0.3 meters, i.e. less than 0.3 cycles. The remaining error term of the ambiguity resolution corresponds to the ionospheric refraction with a value of 0.0580 cycles/TECU (from values in table 1). This term can decrease the success rate, but it is not a critical term at mid-latitudes and at distances below few hundreds of kilometers, where the double differenced STEC values, $\nabla\Delta I$, are typically lower than 10 TECU (see for instance the corresponding values of the analyzed datasets in figure 5).

Step 3. The L1 phase ambiguity is derived from the difference between L1 and the unambiguous wide lane obtained previously. In this step, the main problem is the corresponding ionospheric differential refraction (about 1.9 cycles/TECU), which can produce errors of several cycles at mid-latitudes (see figure 5 with typical values).

In the third step, we apply a similar approach as in the second one, but using the carrier phase differences between the short wavelength and the mid-wavelength, instead of the mid and long ones:

$$\nabla\Delta\hat{N}_1 = \frac{1}{\lambda_1}\nabla\Delta\left(L_1 - L_w + \lambda_w N_w\right) = \nabla\Delta N_1 + \\ -\frac{1}{\lambda_1}\nabla\Delta(\varepsilon_w + m_w - m_1) + \frac{1}{\lambda_1}(\alpha_1 - \alpha_w)\nabla\Delta I \quad (6)$$

In this step, the combination of the carrier phase measurement error and a moderate multipath only introduces again a typical error below 0.2 cycles (see table 1). However, the critical problem here is the ionospheric refraction that could introduce errors greater than .5 cycles (-1.9475 cycles/TECU, equation 6 and values of table 1) also for short baselines (see figure 2). This fundamental limitation can be overcome by computing real-time ionospheric corrections better than 0.26 TECU (i.e. 0.5 cycles*1TECU/1.9475 cycles) to assure the right integer ambiguity estimation. Once the two wide lanes and L1 have been resolved, the resolutions of L2 and L3 immediately follow.

THE REAL-TIME IONOSPHERIC MODEL

To overcome the problem in the third step (i.e. to determine the shortest wavelength ambiguities), we can apply, as in WARTK , a real-time model to estimate the ionospheric differential refraction. This model would be similar to the one used for meter-level augmentation systems such as EGNOS or WAAS, but for sub-decimeter carrier-phase navigation it has to meet higher accuracy requirements. This model is computed from the dual-frequency carrier phase data from fixed network sites, assuming a tomographic description of the sounded ionospheric region, which reduces significantly the mismodelling of the electron content (Hernández-Pajares et al. 1999a-b). With this approach, and the simultaneous determination of tropospheric delays and Lc biases with a geodetic procedure, it is possible to estimate the differential ionospheric refraction with an error below 0.26 TECU, at distances of hundreds of kilometers from the nearest site, under many different ionospheric conditions. This precision implies typical errors below 0.5 cycles in the L1 instantaneous ambiguity fixing at mid- and long distances.

In the case of Wide Area Differential GPS networks, from these real-time Slant Total Electron Content (STEC) corrections obtained by the tomographic model, it is possible, to form the station-satellite double differences, $\nabla\Delta STEC$, with an error below 0.26TECU, and to obtain a second ambiguity (the wide lane) in the reference stations. And, finally, to interpolate to the location of the rover the unambiguous $\nabla\Delta STEC$ with a precision of a few tenths of TECU . If the interpolated value is better than 0.26 TECU, then the rover will be able to solve both ambiguities in real-time. More details on this technique (WARTK) can be found in Colombo et al. (1999) and Hernández-Pajares et al. (2000 a).

FROM WARTK TO WARTK-3

We have extended WARTK, adding the ionospheric modelling and correction to the instantaneous three-carrier phase ambiguity resolution algorithm (TCAR), to medium and long distances (from tens to hundreds of kilometers), and with a minimum of additional computation. The result is WARTK-3. The main improvement is the use of the ionospheric correction in the 3rd TCAR step (in previous section). An improvement made earlier on to the 1st TCAR step will be also implemented in WARTK-3: using the mean of the 3 pseudo-ranges (P1, P2, P3) instead of a single value of Pew, to diminish the effect of the multipath in the extra-wide lane ambiguity resolution (this would be equivalent, in this step, to the ITCAR in single-epoch mode). Ionospheric refraction in P1, P2, or P3 has the same sign, and nearly the same size as in Lew, compared with its long wavelength, so this refraction should virtually cancel out when subtracting a pseudo-range from the extra-wide lane. Finally, an integrity test will be performed using the wide lane and L1 codes to detect jumps in the ambiguity estimation associated with errors in the extra-wide lane ambiguity and wide lane resolution. Indeed, looking at the 2nd and 3rd TCAR steps, equations 5 and 6, it is easy to see that 1 cycle of extra-wide lane ambiguity error produces an error of about 8 cycles in the regular wide lane and each cycle of wide lane error produces about 4 cycles of L1 error. Many times these ambiguity estimation jumps, produced by bad extra-widelane ambiguity determinations due to the pseudorange multipath, are large enough to be detected and filtered out by using the corresponding Pw and P1 pseudo-range combinations With three frequencies, two additional checks should be made to verify: (a) The equal parity (even/odd) of N1-N3 and N1+N3, and of N1-N2 and N1+N2; (b) that before rounding off to the nearest integer number of wide lane wavelengths, Lew-Pew < 0.1 cycle from that integer, and a similar condition on Lw, but substituting the pseudo-range with Lc plus its estimated bias. These are all "geometry-free" checks on the resolved ambiguities. Additional "geometry-dependent" checks have been implemented in the long-range kinematic software (developed by the last author) that we have used in the past (e.g., Colombo et al., 1999, 2000, 2002): The ambiguities are assimilated by the navigation filter as pseudo-observations, so the last check is the null-hypothesis test made on all a posteriori data residuals to either accept or reject the data. As a final precaution, the formal accuracy of a "floated" Lc bias about to be fixed is first taken into account: if it is better than a few cm, and presumably already quite correct, it does not need fixing, and it is not. (The estimation of "floated" Lc biases, whether explicit or implicit, is an integral part of any reliable long-range navigation algorithm based primarily on carrier phase data.) These "geometry-dependent" tests require at least 5 satellites in common view. With only 4 in the simulated data sets, we present here results for the "geometry-free" part of the technique alone.

WARTK-3 could help mitigate significantly a major limitation on our ability to navigate with high precision at long distances (more than 100 km from the nearest reference station). And it complements previous approaches (see table 2).

	ADVANTAGES	**DISADVANTAGES**
TCAR	Low computational load.	Seriously limited by ionospheric refraction.
ITCAR	Improved results by integrating TCAR in a navigation filter.	The ionospheric delay still limits the 3rd ambiguity fixing.
WARTK	Accurate real-time ionospheric modelling, allows precise navigation at hundreds of kilometers from the nearest reference site .	In spite of speeding-up the navigation Kalman filter, a significant convergence time is still needed (5-15 minutes).
WARTK-3	Uses the extra-widelane, and an accurate real-time iono. model to provide single-epoch precise navigation capabilities, and greatly speeding up the convergence of the Navigation Filter to just a few epochs).	

Table 2: Main advantages and disadvantages of the four real-time ambiguity resolution procedures discussed in this work: TCAR, Integrated TCAR, WARTK and WARTK-3 frequencies.

DATA

To prove the feasibility of WARTK-3, we have analyzed several datasets, with simulated airplanes, surface roving users, and fixed sites. We have studied in detail the important case of a receiver on a moving surface vehicle (SUR2) at a distance of e 129 kilometers from a reference site (REF5), under different ionospheric conditions.

The datasets were generated with a modified GNSS satellite signal generator, provided by ESA and produced in the context of a previous funded study (Laboratory Experiment, 2000). The two GPS carriers (at 1575.42 and

1227.60 MHz), and the GLONASS channel 24 carrier (at 1615.50 MHz) were the three frequencies used in the GNSS simulator, with 4 satellites in view for 20 minutes, with the data sampling rate of 1Hz, using all 12 available channels of an AGGA validation receiver. These data are adequate for our real-time ambiguity determination studies, because we are using a geometry-free method, but they are very limited (just 4 satellites) for navigation purposes. Two basic datasets have been considered in this work: P5M0 with maximum signal power and no multipath, and P3M1 with medium power and multipath (see Laboratory Experiment 2000, AGGA Validation 2000 for details). In this last, and more difficult situation, the corresponding multipath for code and carrier phases, mostly affecting steps 1 and 2 respectively of TCAR, reach to more than 4 meters for the pseudo-range, and to more than 5mm for the carrier phase.

In addition to the reference receivers simulated in the datasets (see layout in figure 4), three additional stations (based on existing ones from the IGS network) have been added at distances of more than 200 kilometers to assist the ionospheric modelling, emulating a more realistic situation with a broader network of fixed sites.

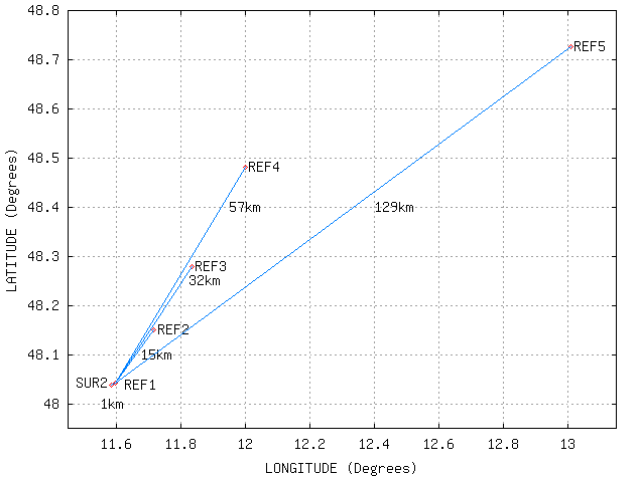

Figure 4: Typical baselines from the roving receiver SUR2 to the five different reference receivers considered in this work.

In the original dataset, the ionospheric values corresponded to night conditions, with negligible effects on baselines shorter than 60 km. In this work, ionospheric refraction values corresponding to the noon of the target day (17 March 2000, in the Solar Max peak) have been generated using an ionospheric climatological model (IRI, Bilitza 1990). These values are about 5 times greater than the Slant Total Electron Content (STEC) values simulated in the original data (based on Klobuchar model at night time). Other values corresponding to additional scenarios (night time, low latitude, high dynamics) have been also generated. In figure 5, it can be seen that the STEC, double-differenced between pairs of satellites and receivers, are larger than 2.7 cm for baselines of 15 kilometers and more, impeding the third ambiguity resolution $\nabla\Delta N_1$ (see equation 6). This was not the case with the ionospheric values generated in the original datasets, corresponding to night values. Indeed, the double differences of the original datasets STEC only exceeded the ambiguity resolution threshold when the more distant reference stations, at 129 km, is considered. This is compatible with the low instantaneous ambiguity resolution success rates reported at such distances by Vollath et al. (2001).

We are going to see in the next section that the application of the real-time tomographic mode to correct ionospheric delays may often reduce this effect below the 0.26 TEC, ensuring the resolution of the ambiguities of all three carrier-phases.

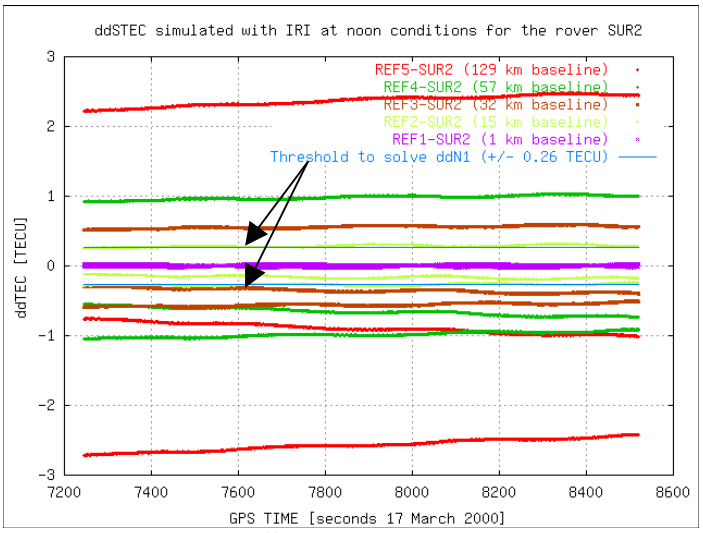

Figure 5: Double differenced Slant Total Electron Content simulated with IRI noon values, $\nabla\Delta I$, for surface roving receiver SUR2, referred to five different reference stations, REF1-5, at distances of 1 to 129 km far.

RESULTS WITH THE MOST DISTANT REFERENCE STATION

We are going to show the results for the more difficult case of the longest baseline: SUR2-REF5, of about 130km (see rover trajectory in figure 6).

Ionospheric filter

First, let us look at the real-time ionospheric filter performance. The estimated versus the true ionospheric delays are shown in figure 7. And, more important for navigation purposes, in figures 8 and 9, one can see the differences (errors) between the double-differenced STEC for the rover according to the model, $\nabla\Delta\hat{I}$, and the true values, $\nabla\Delta I$, obtained from the rover's data. 92% of the values have errors below the threshold limit of 0.26 TECU, for all the receiver datasets corresponding to this baseline. This is accurate enough to be able to resolve the 3 ambiguities in the absence of multipath, and not taking into account the measurement error. Most of the 8% of estimates with errors greater than 0.26TECU come from satellite PRN 26, that is observed at a low elevation and

towards the South, where the highest ionospheric gradients take place (see figure 1). These results could be still slightly improved by adding an additional fifth station to the south of the present network and of the rover.

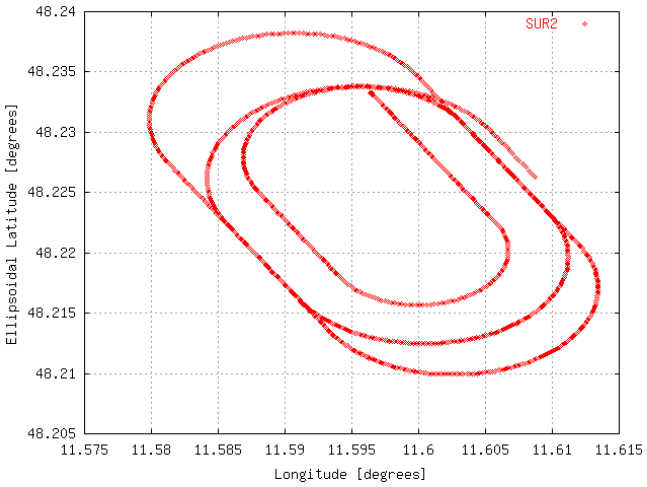

Figure 6: The trajectory of the ground rover SUR2 is shown.

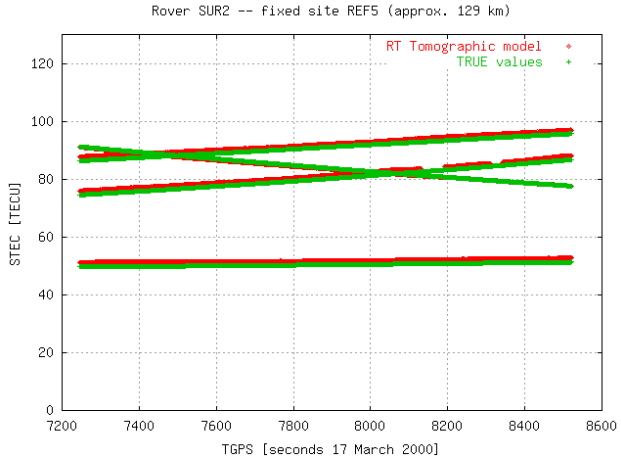

Figure 7: Absolute Slant ionospheric correction (STEC) estimated in real-time with the tomographic model, compared with the true values for the surface roving receiver SUR2.

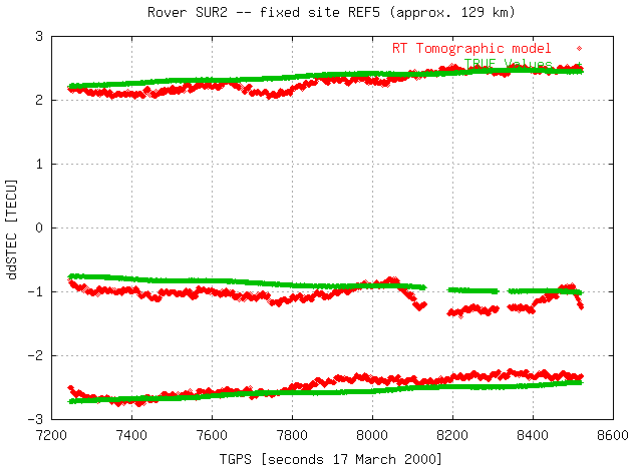

Figure 8: Double differenced STEC estimated in real-time with the tomographic model, compared with the true values for the surface roving receiver SUR2 referred to the most distant receiver, REF5 (about 129 km away from the rover).

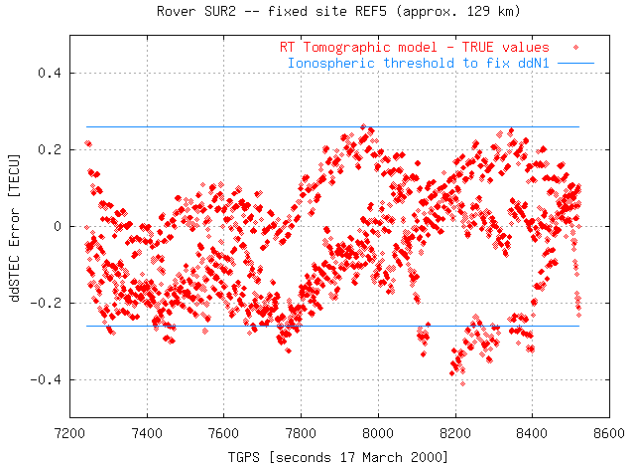

Figure 9: Error in the real-time tomographic determination of the double differenced STEC. More than 92% of the ionospheric estimates present errors below the threshold for successfully resolving the third ambiguity $\nabla\Delta N_1$ (+/- 0.26 TECU).

Ambiguity resolution success

Once the real-time ionospheric corrections are computed and distributed from the reference network to the users, the WARTK-3 algorithm can be applied to estimate and fix in one single epoch the full set of 3 ambiguities per double-difference.

A summary of the main ambiguity resolution results is shown in tables 3 and 4, for the datasets P5-M0 and P3-M1, without and with multipath respectively, where the success in the three TCAR steps is indicated in three cases: (a) without ionospheric corrections, (b) with the corresponding Klobuchar model ionospheric corrections broadcast by the GPS system and (c) with the real-time tomographic ionospheric corrections.

P5-M0 / SUR2-REF5 (≈129km)	Success $\nabla\Delta N_{ew}$	Success $\nabla\Delta N_{w}$	Success $\nabla\Delta N_{1}$
Without ionospheric corrections (TCAR)	100%	100%	0%
TCAR+Klobuchar corrections	100%	100%	33%
Real-time tomographic corrections (WARTK-3)	100%	100%	92%

Table 3: Success relative to the total number of 3834 trials on resolving On-The-Fly the extra-wide lane, wide lane and L1 ambiguities (respectively $\nabla\Delta N_{ew}$, $\nabla\Delta N_{w}$ and $\nabla\Delta N_{1}$) for the roving receiver SUR2 referred to the more distant fixed site (REF5, at about 129 km), and with the ideal dataset P5-M0 (maximum reception power and no multipath). Each row corresponds to cases with different ionospheric corrections: without ionospheric correction (first row), with Klobuchar and real-time tomographic corrections (second and third rows).

It can be seen that the application of the WARTK-3 procedure, combining TCAR and the real-time accurate ionospheric model, allows to increase dramatically the single epoch ambiguity determination success not only in the ideal scenario P5-M0 (from 0 to 92%) but also in the

more difficult one, P3-M1 with multipath (to 92 %, with about 35% using Klobuchar instead of the tomographic corrections).

P3-M1 / SUR2-REF5 (≈129km)	Success $\nabla\Delta N_{ew}$	Success $\nabla\Delta N_{w}$	Success $\nabla\Delta N_{1}$
Without ionospheric corrections (TCAR)	90%	95% (86)	3% (2)
TCAR+Klobuchar corrections	90%	96% (87)	35% (31)
Real-time tomographic corrections (WARTK-3)	90%	96% (87)	92% (79)

Table 4: Same as table 1, but for dataset P3-M1 (medium level of reception power and multipath) and indicating the success only for the observations with the TCAR previous ambiguity successfully solved (in parenthesis, the success rate regarding the total number of observations).

From table 4, it can be seen that one important problem with the P3-M1 datasets, affected by multipath, is the lack of integrity in the TCAR ambiguity estimations, $\nabla\Delta N_{ew}$ and $\nabla\Delta N_{w}$ with about 10% and 4% of erroneous instantaneous determinations, respectively. To increase the integrity, i.e. to decrease the chance of considering erroneous ambiguities, in this case, in the presence of both carrier phase and code multipath, we can use the corresponding wide lane and L1 pseudo-ranges to try to detect potential ambiguity determination errors of the previous longer wavelength ambiguity in the TCAR approach (extra-wide lane and wide lane ambiguities respectively). They are amplified by a factor of about 9 and 4 wavelengths in the extra-wide lane to wide lane and wide lane to L1 determination, respectively (see equations 5 and 6). A summary of the corresponding results is indicated in tables 5 and 6, using the pseudo-ranges and smoothed pseudo-ranges respectively to filter out such large errors.

P3-M1 / SUR2-REF5 (≈129km)	Success $\nabla\Delta N_{ew}$ *	Success $\nabla\Delta N_{w}$ *	Success $\nabla\Delta N_{1}$ *	Availability
Without ionospheric corrections (TCAR)	99%	95% (94)	0(0)%	38%
TCAR+ Klobuchar corrections	99%	97% (96)	33% (32)	38%
Real-time tomographic corrections (WARTK-3)	96%	96% (92)	91% (84)	90%

Table 5: Similar study to that summarized in table 4, but the ambiguity success is here computed after passing the integrity test described in the text. The last column indicates the availability, i.e. % of the 3834 observations passing the previous integrity test with the pseudo-ranges (* percentages of ambiguities computed after passing the integrity test).

It can be seen that with the WARTK-3 approach, a significant increase of integrity (from 79% -table 4- to 91% -table 6-) is attained with a relatively small decrease of 16% of availability (from 100% to 84%) using the smoothed code integrity check. If the single epoch codes are used instead, the integrity is also improved (84%) and with a higher availability (90%). Using the GPS Klobuchar broadcast model, instead of the real-time tomographic corrections, there is a clear worsening of the results, with an almost complete lack of availability.

P3-M1 / SUR2-REF5 (≈129km)	Success $\nabla\Delta N_{ew}$ *	Success $\nabla\Delta N_{w}$ *	Success $\nabla\Delta N_{1}$	Availability
Without ionospheric corrections (TCAR)	100%	100% (100)	0(0)%	0.2%
TCAR+ Klobuchar corrections	100%	100% (100)	37% (37)	0.2%
Real-time tomographic corrections (WARTK-3)	100%	100% (100)	91% (91)	84%

Table 6: Similar study to that summarized in table 5, but using *smoothed pseudo-ranges* - in the integrity test (* percentages of ambiguities computed after passing the integrity test).

Single- epoch rover navigation

The datasets available for this study, in spite of being adequate to work out the instantaneous ambiguity resolution (because this is a "geometry-free" procedure), are very limited to determine the single epoch position. Indeed, just 4 satellites in view are available during 20 minutes of data, in such a way that we had to compute the instantaneous navigation solution for the surface rover SUR2 using the P5-M0 dataset without multipath, and with the highest available signal to noise ratio, in order to assure the minimum number of 4 satellites for navigation. Moreover, the tropospheric delay, orbit errors, etc., for which estimation we would need a 5^{th} satellite at least, has been either substracted or left out. Finally the first 7200 to 7500 seconds approximately, has been avoided in the positioning due to certain carrier phase break patterns. They are potentially due to small receiver measurement problems in this period. With another dataset containing a realistic set of 6 or more satellites (that we hope will be available to us in the near future), these hard limitations to positioning will disappear, providing better geometry (smaller DOP) and the possibility to detect and de-select the satellites (probably at most one, occasionally) presenting ambiguity errors that are revealed while using a navigation filter, or a Receiver Autonomous Monitoring Algorithm, or RAIM (see for instance Parkinson et al. 1996).

The corresponding results with the 4 satellites contained in the P5-M0 dataset are indicated in figures 10. They contain from top to bottom: The pre-fit residuals, and the East, North and Vertical components of the instantaneous positioning error (all in meters) after using WARTK-3.

And, as a reference, the corresponding plots, but with the true ambiguities, are shown in figure 11.

The main features of the $\nabla\Delta L_c$ pre-fit residuals (top plot of figure 10) are the errors around 10 cm associated with one cycle error in L1 (about 8%, as in table 3), that produce single epoch "jump-like" navigation errors, represented also in the second, third and fourth plots of figure 10, and amplified by the corresponding Dilution Of Precision geometric factor (DOP). These bad L1 ambiguity estimates typically affects one double difference of each 3 available per epoch (the minimum number for positioning). In such a way that this error affects 3 times the positioning (about 24% of the epochs), with 76% of time with 3-D errors below 5 cm and the 100% below 21 cm. Although the error distribution is not gaussian, the resulting 3-D RMS is 7 cm, and 3, 5 and 2 cm for the East, North and Vertical components, respectively.

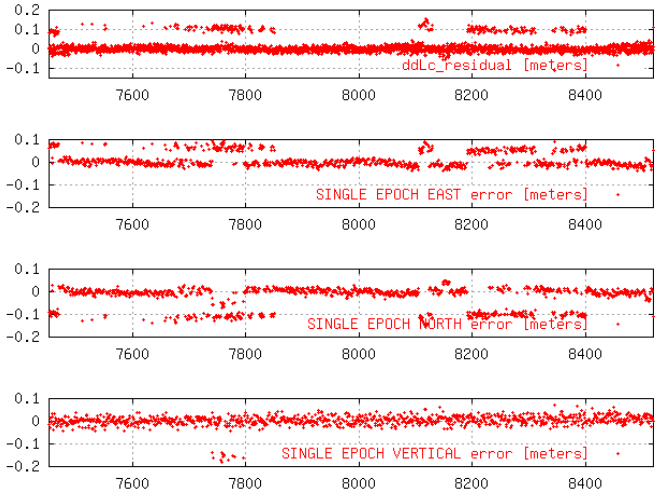

Figure 10: Pre-fit double differenced Lc residual (top plot), and instantaneous (single epoch) navigation errors in East, North and Vertical (up) components (2nd to 4th plots) obtained with WARTK-3 for the rover SUR2 trajectory at about 130 km from the reference site SUR2.

On the other hand, the erroneous positioning components (East, North or Vertical) depend on the geometric information provided by the satellite affected by the L1 one-cycle error. To summarize these results, RMS errors of 1, 1 and 2 cm are obtained for the East, North and Up components respectively, when the ambiguity is well fixed (about 92% of the trials and 77 % of the epochs) and 3, 5 and 2 cm of corresponding RMS errors with the full set of epochs.EMBED

The ionospheric free combination Lc pre-fit residuals and the single-epoch navigation errors, using the true ambiguities, can be seen in figure 11. The amplification of the carrier phase noise is evident, in particular, in the vertical component reaching to about 5 cm of error. This trajectory (with and 3-D RMS of 3cm, and 1, 1 and 2 cm in the North, East and Up components, and 95% levels at about 2, 2 and 4 cm respectively) represents the solution that could be obtained with a real-time filter quite well, instead of the single-epoch solution, after fixing enough ambiguities, from the epoch 50 approximately (figure 10).

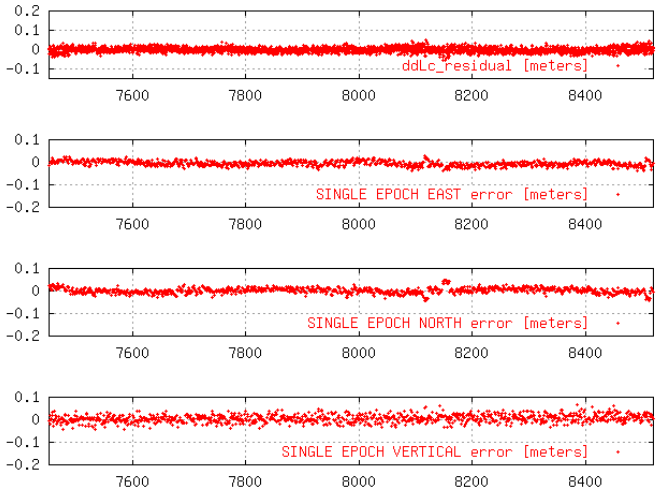

Figure 11: Same as previous figure 10, but for the true ambiguities.

Latency

In order to characterize the impact of latencies in the ionospheric correction (due for instance to the updating design of the model, or to potential problems in comunications), we have considered delays from 1 to 30 seconds in the ionospheric correction computations within the fixed sites network. For each of these delays, the success percentage on achieving the accuracy of 0.26 TECU has been computed: the effect is negligible up to 30 seconds, with success greater than 90%.

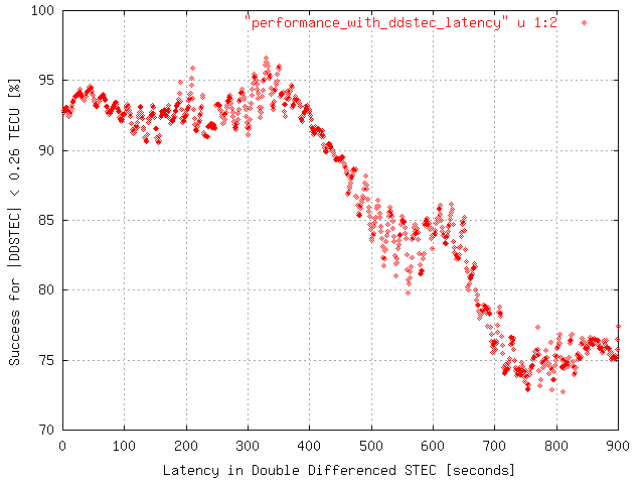

Figure 12: Similar plot to the previous one, but considering common latencies in the reference and rover data..

In figure 12, we have also considered greater latencies for both reference network corrections and rover in such a way that the ionospheric pierce points remain close. It can be seen that the previous result is maintained to about 5 minutes. After this time the success decreases from 90 to 85%. And after 10 minutes, the success decreases to 75%. Note that the jumps correspond to the epochs in which the double differenced STEC variations of each satellite reach

to 0.26 TECU (see figure 8). These numbers can worsen in scenarios with still higher differential ionospheric delay variation. These numbers suggest that at mid-latitude the ionospheric latency is not an issue for WARTK-3 (up to about 5 minutes of latency).

OTHER SCENARIOS

In order to better characterize the WARTK-3 performance, we summarize the results in different scenarios from the point of view of the main problem, the ionosphere, for long baselines. The same set of receivers has been maintained, but simulating ionospheric night conditions (lower values), low latitude (higher values) and high dynamics with a roving aircraft (higher variations).

Night ionospheric conditions

The performance of WARTK-3 in night conditions with small ionospheric delays is still better (100%) than at noon time (92%, last section) as it is expected. If the ionospheric corrections are not applied, just 62% of success is attained in the L1 ambiguity determination.

Lower latitude ionospheric conditions

In this new scenario, we have considered greater ionospheric values, by adopting those corresponding to the South of Europe and North of Africa, at a latitude of about 35 degrees, instead of Central Europe at about 48 degrees (figure 1). The success on providing double difference ionospheric corrections more accurate than 0.26 TECU is still maintained at a relatively high value of about 74%, against 33% using the Klobuchar model or just 3% without correcting the ionospheric delay. This performance could be improved by using the rover ionospheric data as well, as in the experiment summarized in the next sub-section.

Extreme ionospheric condictions, under the equatorial anomalies

We present the first results of real-time ambiguity determination in the Tropics, below the northern equatorial anomaly maximum of the vertical ionospheric delay (see figure 1). To do this, we have simulated the ionospheric conditions at about 22 deg. in latitude over Africa. The absolute STEC values and, the double differenced STEC, are greater than in the mid-latitude case by about 50-100%. To cope with the single-epoch ambiguity resolution at about 130 km from the nearest reference site in this extreme case, we have incorporated, the rover ionospheric data, along with that from the stations, as in other studies mentioned earlier on. The success attained providing accurate ionospheric corrections, after about 10 minutes of filter convergence, is around 80% . This result, compared to 0% with Klobuchar or without ionospheric corrections, is promising, suggesting the feasibility of potential improvements in future studies. Notice that these results are possible because the rover user runs its own ionospheric filter, combining its data with the ionospheric corrections gathered from the reference net.

High dynamics: airplane

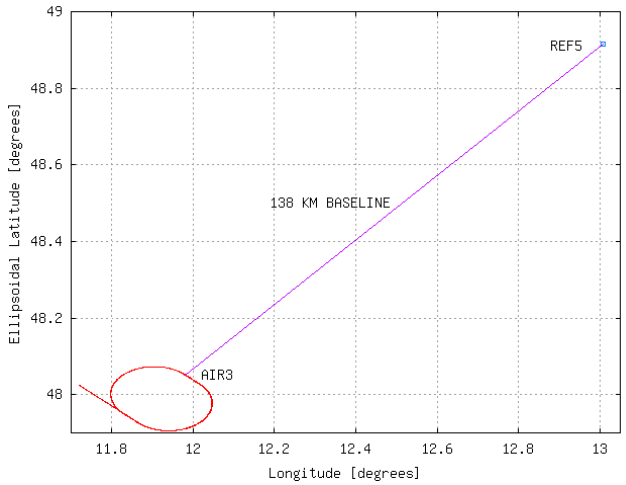

Figure 13: Map for the high dynamic scenario with the aircraft AIR3 flying at the height of 2000 m.

The last ionospheric scenario studied in this work corresponds to the longest baseline at mid-latitude conditions, and with the highest dynamics rover available: an airplane (AIR3) flying at the height of 2000 m, describing ellipses of about 15-20 km in size, about 140 km away from the reference site, REF5 (see corresponding map in figure 13). This cyclic trajectory produces wave-like oscillations in the differential ionospheric delay (figure 15), which makes this scenario more difficult than just with the ground rover SUR2. The errors in the real-time double differenced ionospheric corrections are represented in figure 16, which corresponds to a 73% success for the L1 ambiguity, against 41% and 5% with Klobuchar and without ionospheric corrections. These results could be still improved by adding the rover data as in the case of the experiment mentioned above.

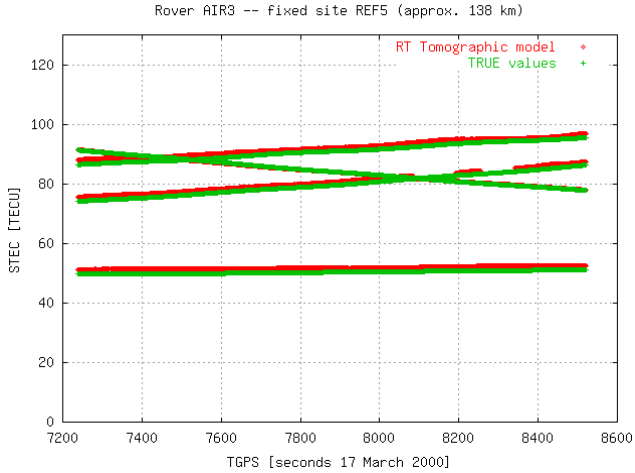

Figure 14: Single epoch estimated STEC and the corresponding true values, in the high dynamics scenario.

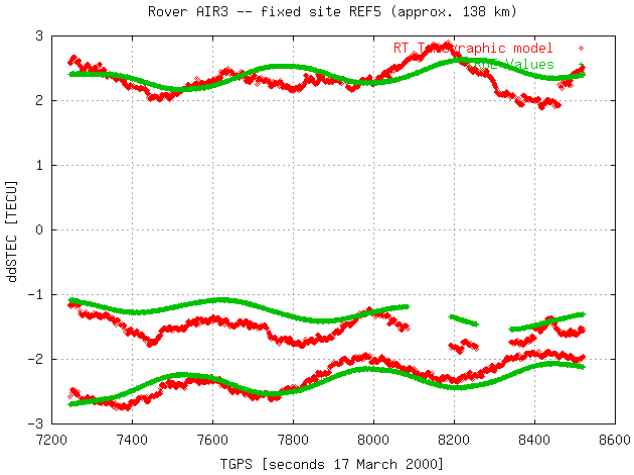

Figure 15: Double differenced STEC instantaneous determination, and the true values, in the high dynamics scenario.

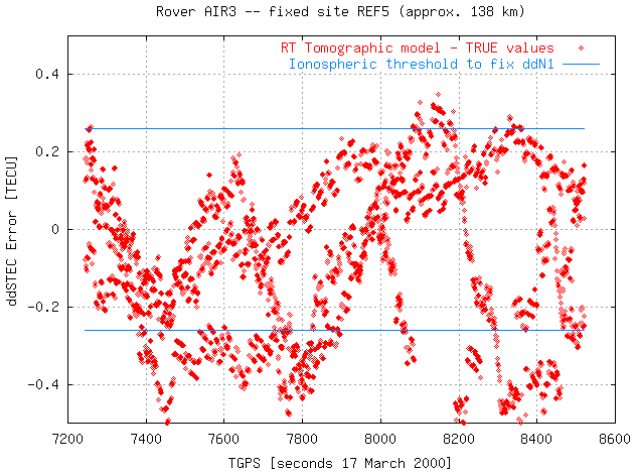

Figure 16: Instantaneous double differenced STEC error in the high dynamics scenario

RESULTS AT DIFFERENT DISTANCES

Finally, we present a summary of the results using different reference stations, indicated in figure 17. The baselines range from 1 km to about 130 km for dataset P3M1, and the generated data include multipath effects. Indeed, the relative success solving $\nabla\Delta N_1$ (when successful wide lane ambiguity occurs), are represented as a function of the distance in figure 17, using the datasets with medium power reception level, multipath, and IRI values to simulate the ionospheric delays. It can be seen that the success decreases from 100% at 1 km to about 50% at 15 km, and near 0% at 32 km, if no ionospheric corrections are considered. However, the inclusion of real-time or Klobuchar model estimates of the ionospheric corrections maintain the success above the 95% for distances of less than 60 km. For the longest baseline (at a mean distance of 129km), only the tomographic model maintains the success above 90%, in contrast with less than 40% provided by the Klobuchar model.

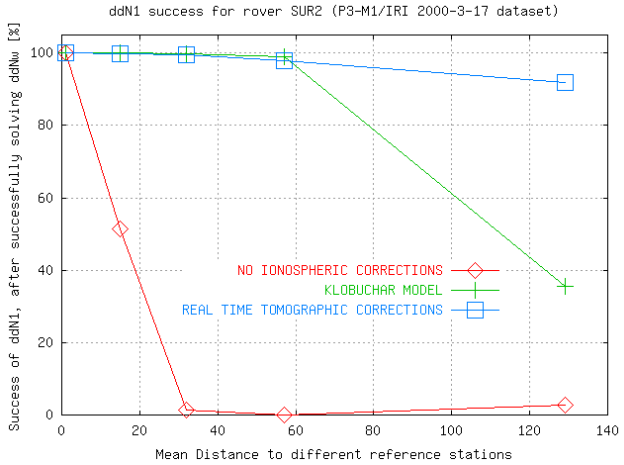

Figure 17: Relative success of $\nabla\Delta N_1$ in the roving surface receiver SUR2, as a function of the distance to the reference station, computed from the P3-M1 dataset.

CONCLUSIONS

The WARTK-3 technique, combining the Three Carrier Phase Ambiguity Resolution procedure (TCAR) with the real-time tomographic determination of the ionospheric corrections, promises the following important improvements in ambiguity resolution and precise navigation, at mid-latitudes and long distances (more than 100 km):

- From an instantaneous (single epoch) success rate of about 60% or less in previous works (such as Vollath et al. 1998, with night-time conditions), to about 90% at distances of more than 100km, and in difficult conditions for the ionospheric modelling (noon in Solar Maximum).
- Maintaining high performance even with latencies of up to 5 minutes in the ionospheric corrections.
- The corresponding navigation, in spite of the limited number of 4 satellites available in the datasets can be done instantaneously, in single-epoch mode, with RMS of 3, 5 and 2 cm in East, North and Vertical components (about 6, 10 and 4 cm at 95%).
- The good performance has been also checked in other difficult ionospheric cases, such as low latitude and high dynamics scenarios.

Additional improvements can be obtained in future work by:

(1) Working with a more realistic, and higher, number of satellites, than the four available in the datasets used in this work, would significantly improve the navigation quality.

(2) Using a long-range navigation filter that estimates rover position simultaneously with error in the tropospheric refraction corrections, errors in the broadcast or other predicted GPS orbits, and floated Lc ambiguities as in our fully implemented WARTK technique.

(3) Combining the ionospheric corrections computed in the reference network with the rover data in an

ionospheric user filter, such as in the case of tropical ionospheric conditions.

(4) Adding more reference stations for the ionospheric determination, to have a better coverage of the sky.

(5) In cases where it is possible to wait a minute or two before the ambiguities are resolved, the chances of successful resolution could be increased considerably by using the averages of several epochs to reduce the effect of noise and multipath, as we have done in some of our past work with GPS.

As the main conclusion, the results of this study suggest that using a real-time tomographic model of the ionosphere, it should be feasible to have instantaneous and full ambiguity resolution, achieving sub-decimeter precise navigation, at distances of more than 100 km, with future three-frequency systems such as GALILEO and the modernized GPS.

ACKNOWLEDGEMENTS

This work has been performed under ESA/ESTEC Contract Number 15453/01/NL/Lv, being Alberto García-Rodríguez the contractor manager.

REFERENCES

AGGA Validation, "Test Setup" and "User Manual", Austrian Aerospace under ESA contract No. 12782/98/NL/GD, Doc. No. OCC-TNT-0026-AAE, May 18, 2000.

Bar-Sever, Y., R. Muellerschoen, A. Reichert, M. Vozoff and L. Young, NASA's Internet Based Global Differential GPS System, 1st ESA Workshop on Satellite Navigation User Equipment Technologies, ESTEC, Nordwijk, The Netherlands, December 2001.

Bierman, G.J., Factorization Methods for Discrete Sequential Estimation, Vol. 128 in Mathematics in Science and Engineering, Academic Press, New York, 1977.

Billitza D., International Reference Ionosphere 1990, URSI/COSPAR, NSSDC/WDC-A-R&S 90-22, 1990.

Colombo, O.L., M. Hernández-Pajares, J.M. Juan, J. Sanz and J. Talaya, Resolving carrier-phase ambiguities on-the fly, at more than 100 km from nearest site, with the help of ionospheric tomography, ION GPS'99, Nashville, USA, September 1999.

Colombo O.L., Hernández-Pajares M., Juan J.M. and Sanz J., Ionospheric Tomography Helps Resolve GPS Ambiguities On-the-Fly At Distances of Hundreds of Kilometers During High Geomagnetic Activity, Position Location and Navigation Symposium (PLANS 2000 IEEE conference), San Diego (USA), March 2000.

Colombo, O.L., Hernández-Pajares M., Juan J.M. and Sanz J., Wide-Area, Carrier-Phase Ambiguity Resolution Using a Tomographic Model of the Ionosphere, "Navigation", in print, 2002.

Harris, R.A.: Direct Resolution of Carrier-Phase Ambiguity by 'Bridging the Wavelength Gap', ESA Publication "TST/60107/RAH/Word", 2/1997.

Hernández-Pajares M., J.M. Juan and J. Sanz, New approaches in global ionospheric determination using ground GPS data, Journal of Atmospheric and Solar Terrestrial Physics. Vol 61, 1237-1247, 1999a.

Hernández-Pajares M., J.M. Juan, J. Sanz and O.L. Colombo, Precise ionospheric determination and its application to real-time GPS ambiguity resolution, Institute of Navigation ION GPS'99, Nashville, Tennessee, USA, September 1999b.

Hernández-Pajares, M., J.M. Juan, J. Sanz and O.L. Colombo, Application of ionospheric tomography to real-time GPS carrier-phase ambiguities resolution, at scales of 400-1000 km, and with high geomagnetic activity, Geophysical Research Letters, 27, 2009-2012, 2000a.

Hernández-Pajares, M., J.M. Juan, J. Sanz, O. Colombo, H. Van der Marel, Real-time integrated water vapor determination using OTF carrier-phase ambiguity resolution in WADGPS networks, ION GPS'2000, Salt Lake City, September 2000b.

Hernández-Pajares, M., J.M. Juan, J. Sanz, O.L. Colombo, and H. van der Marel, A new strategy for real-time Integrated Water Vapour determination in WADGPS networks, Geophysical Research Letters, 28, 3267-3270, 2001.

Hernández-Pajares, M., J.M. Juan, J. Sanz, O.L. Colombo, Tomographic modeling of GNSS ionospheric corrections: Assessment and real-time applications, ION GPS'2001, Salt Lake, USA, September 2001b.

Hernández-Pajares, M., J.M. Juan, J. Sanz, O.L. Colombo, Improving the real-time ionospheric determination from GPS sites at Very Long Distances over the Equator, Journal of Geophysical Research, in press, 2002.

Jung, J., P.Enge, B.Pervan, Optimization of Cascade Integer Resolution with Three Carrier GPS Frequencies, Proceedings of the ION-GPS 2000.

Laboratory Experiment On Carrier Phase Positioning Techniques for GNSS 2 (TCAR-Test). Technical Note "Familiarization with Test Equipment" and "Generation of Scenarios", Spectra Precision Terrasat GmbH, Germany, under ESA contract No. 12406/77/NL/DS Rider 1, Issue 1, Revision 2, Sept. 2000.

Parkinson B.W., J.J.Spilker, Global Positioning System: Theory and Applications, Progress in Astronautics and Aeronautics, Vol. 163 and 164, A.I.A.A. Inc, 1997

Vollath, U., S. Birnbach, H. Landau, J.M. Fraile-Ordoñez, M. Martin-Neira, Analysis of Three-Carrier Ambiguity Resolution (TCAR) Technique for Precise Relative Positioning in GNSS-2, Proceedings of the ION-GPS 1998.

Vollath, U., E. Roy, Ambiguity Resolution using Three Carriers - Performance Analysis using "Real" Data, GNSS Symposium, Seville, May 2001.